



Stuart, F. M., Mark, D. F., Gandanger, P., and McConville, P. (2016) Earth-atmosphere evolution based on the new determination of Devonian atmosphere Ar isotopic composition. *Earth and Planetary Science Letters*, 446, pp. 21-26. (doi:[10.1016/j.epsl.2016.04.012](https://doi.org/10.1016/j.epsl.2016.04.012))

This is the author's final accepted version.

There may be differences between this version and the published version. You are advised to consult the publisher's version if you wish to cite from it.

<http://eprints.gla.ac.uk/119126/>

Deposited on: 16 May 2016

Enlighten – Research publications by members of the University of Glasgow
<http://eprints.gla.ac.uk>

1 **Earth-atmosphere evolution based on new determination of Devonian**
2 **atmosphere Ar isotopic composition**

3

4

5 Finlay M. Stuart*, Darren F. Mark, Pierre Gandanger & Paul McConville

6 Isotope Geoscience Unit, Scottish Universities Environmental Research Centre, East Kilbride

7 G75 0QF, United Kingdom

8

9 *Corresponding author e-mail: fin.stuart@glasgow.ac.uk

10

11

12

13 Main text: 3,082 words

14

15

16

17

18

19 **Abstract**

20 The isotopic composition of the noble gases, in particular Ar, in samples of ancient
21 atmosphere trapped in rocks and minerals provide the strongest constraints on the timing
22 and rate of Earth atmosphere formation by degassing of the Earth's interior. We have re-
23 measured the isotopic composition of argon in the Rhynie chert from northeast Scotland
24 using a high precision mass spectrometer in an effort to provide constraints on the
25 composition of Devonian atmosphere. Irradiated chert samples yield $^{40}\text{Ar}/^{36}\text{Ar}$ ratios that
26 are often below the modern atmosphere value. The data define a $^{40}\text{Ar}/^{36}\text{Ar}$ value of 289.5
27 ± 0.4 at $\text{K}/^{36}\text{Ar} = 0$. Similarly low $^{40}\text{Ar}/^{36}\text{Ar}$ are measured in un-irradiated chert samples.
28 The simplest explanation for the low $^{40}\text{Ar}/^{36}\text{Ar}$ is the preservation of Devonian
29 atmosphere-derived Ar in the chert, with the intercept value in ^{40}Ar - ^{39}Ar - ^{36}Ar space
30 representing an upper limit. In this case the Earth's atmosphere has accumulated only
31 3% ($5.1 \pm 0.4 \times 10^{16}$ mol) of the total ^{40}Ar inventory since the Devonian. The average
32 accumulation rate of $1.27 \pm 0.09 \times 10^8$ mol $^{40}\text{Ar}/\text{year}$ overlaps the rate over the last 800
33 kyr. This implies that there has been no resolvable temporal change in the outgassing
34 rate of the Earth since the mid-Palaeozoic despite the likely episodicity of Ar degassing
35 from the continental crust. Incorporating the new Devonian atmosphere $^{40}\text{Ar}/^{36}\text{Ar}$ into the
36 Earth degassing model of Pujol et al (2013) provides the most precise constraints on
37 atmosphere formation so far. The atmosphere formed in the first ~ 100 Ma after initial
38 accretion during a catastrophic degassing episode. A significant volume of ^{40}Ar did not
39 start to accumulate in the atmosphere until after 4 Ga which implies that stable K-rich
40 continental crust did not develop until this time.

41

42 **1. Introduction**

43 The concentration of the noble gases (He, Ne, Ar, Kr and Xe) in the main terrestrial
44 reservoirs (mantle, crust and atmosphere) are not affected by the chemical and
45 biological processes that govern the distribution of the reactive volatile elements. The
46 presence of both stable and radiogenic noble gas isotopes can be used to provide
47 temporal constraints on the outgassing history of the solid Earth and the age of the
48 atmosphere. Consequently they have proved to be key tracers of the origin and
49 evolution of the atmospheres of the terrestrial planets (e.g. Turcotte and Schubert,
50 1988).

51 The origin of the Earth's atmosphere has been critical in the understanding evolution of
52 terrestrial planets. It has been recognised for many decades that the Earth's atmosphere
53 is secondary in origin, a consequence of the outgassing of the planetary interior, rather
54 than capture of solar nebula gases (Brown, 1949). Models of atmosphere growth are
55 largely based on the noble gas isotope composition of the present day mantle, crust and
56 atmosphere. The earliest models proposed that the atmosphere formed as a result of
57 slow, continuous outgassing of the Earth's interior (Turekian, 1959). The low
58 concentration of stable (primordial) noble gas isotopes in mantle rocks compared to
59 primitive chondritic meteorites led to the conclusion that Earth must be strongly
60 outgassed. Subsequent studies of Ar isotopes in Earth interior permitted the
61 development of two-stage outgassing history; an extensive outgassing event soon after
62 Earth accretion was followed by slow continuous degassing (Fanale, 1971; Hamano and
63 Ozima, 1978). The early models were predicated on the assumption that the
64 atmosphere formed by outgassing of only the crust and upper mantle where the deep
65 mantle did not outgas significantly, and remained convectively isolated from the upper
66 mantle (e.g. Allègre et al. 1986/87; 1996). Subsequent modelling demonstrated that the
67 complete outgassing of an upper mantle down to the 670 km seismic discontinuity cannot

68 provide all the ^{40}Ar in the atmosphere (e.g. Davies, 1999). The measurement non-
69 atmospheric Ne and Ar isotope compositions in basalts from intra-plate volcanoes (e.g.
70 Honda et al., 1993; Burnard et al. 1994) led to the recognition that the lower mantle
71 below 670 km cannot have remained convectively isolated for all of Earth history (e.g.
72 Porcelli and Wasserburg, 1995; O’Nions and Tolstikhin, 1996). Recent Earth outgassing
73 models incorporate some degree of volatile loss from the deep mantle (e.g. Gonnerman
74 and Mukhopadhyay, 2009), but the extent to which the deep Earth is degassed, and the
75 source and location of primordial noble gases in Earth’s interior remain unresolved (see
76 discussion in Starkey et al. 2009).

77 While the isotopic composition of noble gases in modern terrestrial reservoirs is well
78 established, the time-integrated rate of mass transfer between these reservoirs, as well
79 as the rate of transfer of primordial and radiogenic volatiles, is much less well
80 constrained (e.g. Farley et al. 1995; Stuart and Turner 1998). The determination of the
81 isotopic composition of noble gases in ancient atmosphere provides a first order test of
82 the degree and rate of gas and mass transfer processes. However, the ubiquity of
83 contaminating modern atmosphere, and the ingrowth of radiogenic isotopes in minerals
84 after crystallisation, severely hampers the precise determination of these signals. Despite
85 this, a low $^{40}\text{Ar}/^{36}\text{Ar}$ component appears to have been incorporated in several ancient
86 rocks and minerals (e.g. Cadogan, 1977; Hanes et al. 1985; Rice et al. 1994; Pujol et al.
87 2013). These values are consistent with the incorporation and retention of ancient
88 atmospheric Ar, although it usually relies on a correction for radiogenic ^{40}Ar ingrowth after
89 mineral or rock formation. The difficulty in explaining systematically low $^{40}\text{Ar}/^{36}\text{Ar}$ by any
90 other mechanism, however, indicates that it is clearly a fruitful avenue for constraining
91 the Earth outgassing history.

92 The Devonian hydrothermal Rhynie chert from northeast Scotland is probably the most
93 thoroughly studied material that may preserve an ancient atmospheric Ar signal. The

94 first detailed study yielded an initial $^{40}\text{Ar}/^{36}\text{Ar} = 291.0 \pm 1.6$ which, it was argued,
95 represented the value of Devonian atmosphere (Cadogan, 1977). Although this value
96 was consistent with what would be expected for catastrophic early Earth degassing (e.g.
97 Turner, 1989) the veracity of the measurements failed to convince some at the time (see
98 Ozima and Podosek, 1983). Subsequent intensive study replicated the low $^{40}\text{Ar}/^{36}\text{Ar}$
99 (291.1 ± 0.6 ; Rice et al. 1994). However, as with the initial study, this work yielded no
100 gas extraction steps with $^{40}\text{Ar}/^{36}\text{Ar}$ ratios that were unequivocally lower than the present
101 day atmospheric value and the presence of palaeo-atmospheric Ar relied on the (not
102 unreasonable) assumption that radiogenic ^{40}Ar was present to some degree in all gas
103 extraction steps. High precision determinations have been made of the isotope
104 composition of atmospheric argon trapped in samples of Antarctic ice dating back several
105 hundred thousand years (Bender et al. 2008). These data require an average modern
106 outgassing rate of 1.1×10^8 mol $^{40}\text{Ar}/\text{year}$. This rate is broadly consistent with, and more
107 precise than, the long-term average calculated from the measurements of Rhynie chert.
108 Most recently a low $^{40}\text{Ar}/^{36}\text{Ar}$ trapped in Archaean hydrothermal quartz from 3.5 Ga
109 Pilbara craton, Western Australia (Pujol et al. 2013) has been used to place constraints
110 on the rate of atmosphere degassing early in Earth history, which has implications for the
111 timescale of formation of continental crust.

112 Several factors warrant a re-assessment of the possibility that the Rhynie chert is a
113 repository of ancient atmospheric noble gases. Recent improvements in multi-collector
114 noble gas mass spectrometers allows for high precision Ar isotope measurements (Mark
115 et al. 2010). The re-determination of the Ar isotope composition of the modern
116 atmosphere (see Mark et al. 2011a for discussion) means that fractionation in the mass
117 spectrometer can be correctly determined, and an appropriate correction for trapped
118 modern air can be made. Finally, a better understanding of the petrology of the Rhynie
119 chert (e.g. Baron et al. 2004) means that potentially problematic components of the rock,

120 e.g. detrital clay, can be avoided. Here we present new determinations of the $^{40}\text{Ar}/^{36}\text{Ar}$ of
121 the Rhynie chert in an effort to determine isotopic composition of the Devonian
122 atmosphere. The new value for Devonian air is incorporated into the Earth degassing
123 model developed by Pujol et al. (2013) and is used to place constraints on the
124 degassing history of the Earth.

125

126 **2. Samples and analytical methods**

127 Argon isotopes have been measured in mg-sized chips of irradiated and un-irradiated
128 pristine siliceous sinter from a single specimen of Rhynie chert. Samples were selected
129 specifically in order to avoid entrained fine-grained sediment, minimising potential issues
130 resulting from the recoil of K-derived ^{39}Ar . We specifically targeted the siliceous sinter
131 that developed on the surface and cooled in direct exposure to the Devonian
132 atmosphere. Detailed descriptions of the Rhynie chert are given elsewhere (e.g. Rice et
133 al. 1994; Baron et al. 2004). Nine samples were irradiated for 100 hours in the Cd-lined
134 nuclear reactor at McMaster, Canada. Eight of these samples were incrementally heated
135 in 5 steps using a 50 W CO_2 laser in an attempt to selectively remove absorbed modern
136 atmospheric Ar and release palaeo-atmospheric Ar. One sample was fused in a single
137 step. Biotite from the Mount Dromedary monzonite (GA1550, 98.8 ± 0.5 Ma, Renne et
138 al. 1998) was used as a neutron fluence monitor. Details of the irradiation parameters
139 are given in the Supplementary Information. Samples were outgassed at $\sim 80^\circ\text{C}$ in a Cu
140 laser pan for 10 days prior to analysis in order to remove adhering atmospheric Ar. The
141 extraction, purification and analysis procedures were similar to those described in Mark
142 et al. (2011b).

143 Argon isotopes were measured in 12 unirradiated chips of Rhynie chert. The gas
144 extraction procedure and purification was identical to that applied to the irradiated chips.

145 Five samples were incrementally heated in three steps, and seven were fused in a single
146 step.

147 Argon isotope abundances and ratios were determined using a GVI ARGUS multiple-
148 Faraday collector mass spectrometer using established laboratory procedures (Mark et
149 al. 2010). System blanks were measured after every two measurements of unknowns.
150 Average blank measurements for the entire run sequence were used to correct raw peak
151 intensities. Mass discrimination ($1.0059 \pm 0.0009/\text{amu}$) was determined by repeated
152 measurement of air pipettes during the period of analysis (following every five analyses).

153

154 **3. Results**

155 The data from the irradiated and unirradiated samples are compiled in the
156 Supplementary Information. Argon in the samples likely derives from four sources;
157 modern air, Devonian air, ^{40}Ar generated from ^{40}K decay and “excess” ^{40}Ar in the
158 hydrothermal fluids (see Rice et al. 1994 for review). These components can best be
159 resolved using the analyses of irradiated samples. In ^{40}Ar - ^{39}Ar - ^{36}Ar space the data define
160 a triangular region that appears to have a well-defined lower bound (Figure 1). The data
161 that plot above the lower bound may be affected by a small contribution of excess ^{40}Ar
162 that originates in the trapped hydrothermal fluid. They are statistically insignificant. A
163 correlation between Ca-derived ^{37}Ar and K-derived ^{39}Ar (SI Table 1) indicates that a Ca-
164 and K-bearing mineral or fluid inclusion phase is present in the chert. While a trapped
165 fluid phase is present in the Rhynie chert (Rice et al. 1994), the presence of detrital clay
166 minerals cannot be ruled out. ^{39}Ar recoil from clays can perturb the Ar isotope
167 systematics but there is no clear evidence of the effect in this case (Figure 1).

168 Following the protocol established by earlier studies (Cadogan 1977; Rice et al. 1994;
169 Pujol et al. 2013) we use a conventional isochron to determine the palaeo-atmosphere

170 $^{40}\text{Ar}/^{36}\text{Ar}$. The majority of the data define a statistically robust isochron that has a slope
171 consistent with a $^{40}\text{Ar}/^{39}\text{Ar}$ age of 380 ± 30 Ma (see Figure 1 for description). This
172 overlaps the more precise $^{40}\text{Ar}/^{39}\text{Ar}$ age (408 ± 2 Ma) determined on adularian feldspar
173 from a feeder vein beneath the Rhynie chert body (Mark et al. 2011b; 2013). The
174 intercept of the y-axis at $K/^{36}\text{Ar} = 0$ is consistent with the trapped argon having a $^{40}\text{Ar}/^{36}\text{Ar}$
175 of 289.5 ± 0.4 . This is significantly lower than modern air value and is consistent with,
176 though significantly lower than, previous studies (Cadogan 1977; Rice et al. 1994).

177 In contrast to these earlier studies, the $^{40}\text{Ar}/^{36}\text{Ar}$ of many individual measurements are
178 lower than the modern air value, providing some confidence that the sub-atmospheric
179 $^{40}\text{Ar}/^{36}\text{Ar}$ is trapped in the chert, and is not an artifact of disturbance to the K- ^{40}Ar system.
180 There is no systematic relationship between ^{40}Ar or K-derived ^{39}Ar with Cl-derived ^{37}Ar
181 produced during the irradiation process that might be indicative of the low $^{40}\text{Ar}/^{36}\text{Ar}$
182 component residing in hydrothermal fluid inclusions. Further the analyses that appear to
183 contain small excesses of ^{40}Ar (yellow data in Figure 1) do not have a clear relationship
184 with Cl-derived ^{38}Ar that might indicate an origin in hydrothermal fluid inclusions (e.g.
185 Turner, 1988).

186 It is tempting to invoke a palaeo-atmospheric source for the sub-atmospheric $^{40}\text{Ar}/^{36}\text{Ar}$
187 ratios in the chert. However, we must exclude alternative possibilities. The unirradiated
188 samples reproduce the low $^{40}\text{Ar}/^{36}\text{Ar}$ measured in the irradiated samples while $^{38}\text{Ar}/^{36}\text{Ar}$
189 ratios are within analytical uncertainty of the atmospheric composition (Figure 2 and
190 Table S12). This provides no indication for the presence of fractionated modern air Ar in
191 the chert, and rules out significant mass fractionation during analysis, or a significant
192 contribution of isobaric interferences of $^{12}\text{C}_3^+$ or H^{35}Cl^+ at $^{36}\text{Ar}^+$. The samples are from
193 boreholes several tens of meters underground. Along with the absence of excess ^{38}Ar
194 (Figure 2), this rules out cosmogenic ^{36}Ar as an explanation for the low $^{40}\text{Ar}/^{36}\text{Ar}$.

195 Following the earlier studies (Cadogan, 1977; Rice et al. 1994) we conclude that the
196 Rhynie chert has trapped Ar derived from ancient atmosphere. Assuming that it was
197 incorporated at the time of chert formation, it reflects the signature of Devonian
198 atmosphere. The likelihood that a small contribution of modern air-derived Ar is present
199 in some of the analyses used to define the isochron implies that the $^{40}\text{Ar}/^{36}\text{Ar}$ intercept
200 value (289.5 ± 0.4 ; Figure 1) is an upper limit of the Devonian atmosphere.

201

202 **4. Discussion**

203 **4.1 Earth outgassing since Devonian**

204 The $^{40}\text{Ar}/^{36}\text{Ar}$ of the Devonian atmosphere in this study (289.5 ± 0.4) is 3.1 ± 0.2 % lower
205 than the best estimate of present day air (298.8 ± 0.5 ; Lee et al. 2008). Previous studies
206 of Rhynie chert have reported trapped $^{40}\text{Ar}/^{36}\text{Ar}$ ratios of around 291 (Cadogan, 1977;
207 Rice et al. 1994). These determinations were made on instruments that had been
208 calibrated against atmospheric Ar assuming $^{40}\text{Ar}/^{36}\text{Ar} = 295.5 \pm 0.5$ determined by Nier
209 (1956). In these cases the trapped palaeo-atmospheric $^{40}\text{Ar}/^{36}\text{Ar}$ is $\sim 1.5\%$ lower than the
210 present day atmosphere value. If our new measurement represents atmosphere trapped
211 at the time of chert formation, the post-Devonian degassing rate is approximately twice
212 the rate determined previously, approximately 3% lower than modern air (Cadogan,
213 1977; Rice et al. 1994).

214 For a modern global atmospheric ^{40}Ar inventory of 1.65×10^{18} moles (Hamano and
215 Ozima, 1978), our data imply that the atmosphere has accumulated $5.1 \pm 0.4 \times 10^{16}$
216 moles of ^{40}Ar in the last 404 million years. This equates to an average degassing rate of
217 $1.27 \pm 0.09 \times 10^8$ mol $^{40}\text{Ar}/\text{year}$. This is slightly in excess of, but overlaps within 1σ
218 uncertainty, the Quaternary accumulation rate of ^{40}Ar in the atmosphere derived from

219 measurements of Greenland and Antarctic ice cores in the last 800,000 years (1.1 ± 0.1
220 $\times 10^8$ mol $^{40}\text{Ar}/\text{year}$; Bender et al. 2008).

221 The bulk of the atmosphere ^{40}Ar flux outgases from the continental crust as a result of
222 mineral breakdown during chemical weathering and metamorphism, and diffusion from
223 deep crustal rocks (Bender et al. 2008). The short-term outgassing rate of the crust is
224 expected to vary according to the proportion of ancient (^{40}Ar -rich) basement rocks that is
225 available for weathering, and the intensity of metamorphism. The apparent overlap of the
226 short-term (<1 million years) and the long-term (400 million years) outgassing rates
227 suggests that the time constant for Ar outgassing from the crust may be so long as to
228 minimize the effect of large scale, episodic geological processes such as orogenesis.

229

230 **4.2 Degassing of the early Earth**

231 Recently Pujol et al. (2013) reported the Ar isotope composition of hydrothermal quartz in
232 Archaean-aged metasedimentary rocks from the Pilbara craton, Western Australia.
233 Although no individual incremental heating steps yielded a measured $^{40}\text{Ar}/^{36}\text{Ar}$ ratio
234 below the modern atmosphere value, when corrected for ^{40}K -decay the individual steps
235 extrapolated to a $^{40}\text{Ar}/^{36}\text{Ar}$ value of 143 ± 24 (1σ). They argued that this represents the
236 best estimate of the isotopic composition of Ar in the Earth atmosphere at 3.5 Ga (Pujol
237 et al. 2013). Using a first-order rate box model similar to the one developed by Hamano
238 and Ozima (1978) they used this palaeo-atmospheric $^{40}\text{Ar}/^{36}\text{Ar}$ to constrain the evolution
239 of the atmosphere $^{40}\text{Ar}/^{36}\text{Ar}$ and thus place limits on the timing of crust formation and
240 degree of crust degassing. How this data constrains the evolution of atmosphere
241 $^{40}\text{Ar}/^{36}\text{Ar}$ since 4.56 Ga and 500 Ma is shown in Figures 2a and 2b respectively, along
242 with our new determination of Devonian atmosphere $^{40}\text{Ar}/^{36}\text{Ar}$. The new data plots well

243 within the limits predicted by the Pujol et al (2013) degassing model (Figure 2b),
244 confirming the veracity of their data and model.

245 Here we incorporate our new data into the atmospheric Ar isotope evolution model
246 established by Pujol et al. (2013). The model parameters are similar to Pujol et al.
247 (2013) (see Supplementary Information for description) with the exception that we fix the
248 current ^{40}Ar degassing rate at $1.2 \times 10^8 \text{ mol } ^{40}\text{Ar}/\text{year}$, in line with this work and Bender et
249 al. (2008), rather than the lower degassing rate derived from the earlier measurement of
250 palaeoatmospheric Ar in Rhynie chert ($6.6 \pm 3.3 \times 10^7 \text{ mol } ^{40}\text{Ar}/\text{year}$; Cadogan, 1977).
251 This makes no significant difference to the Ar outgassing curves that we derive, or to the
252 conclusions of this work. The evolution of the atmospheric $^{40}\text{Ar}/^{36}\text{Ar}$ has been determined
253 for a single crust growth model where only the degree of crustal degassing has been
254 varied.

255 The Earth outgassing histories that predict the maximum and minimum Devonian
256 atmosphere $^{40}\text{Ar}/^{36}\text{Ar}$ defined by our new measurements, and those of Pujol et al.
257 (2013), are shown in Figure 2. The new model curves are within the envelope of
258 degassing histories that describe the earlier data. However, the new model predicts a
259 narrower range of atmospheric $^{40}\text{Ar}/^{36}\text{Ar}$ (120 to 130) at 3.5 Ga than extrapolated from
260 the measurement of the Pilbara hydrothermal quartz (119 to 167; Pujol et al., 2013)
261 (Figure 2b). This higher precision determination of early Earth atmosphere $^{40}\text{Ar}/^{36}\text{Ar}$ ratio
262 provides a significantly improved constraint on the early degassing history. Our new
263 model predicts atmospheric $^{40}\text{Ar}/^{36}\text{Ar}$ at 3.5 Ga that are at the lower end of the range
264 measured by Pujol et al. (2013). The slightly higher $^{40}\text{Ar}/^{36}\text{Ar}$ of Pujol et al (2013) may
265 reflect the presence of a small contribution of modern atmospheric Ar in their
266 measurements.

267 The refined atmospheric Ar evolution model (Figure 2a and b) confirms the need for
268 outgassing of a significant proportion of the Earth's primordial volatile inventory within
269 100 million years or so of accretion (e.g. Fanale, 1971; Hamano and Ozima, 1978;
270 Turner, 1989). This is significantly earlier than the Late Heavy Bombardment (3.8 - 4.1
271 Ga) (Gomes et al. 2005) and rules out wholesale loss of the early atmosphere during this
272 process. The catastrophic outgassing overlaps the time of formation of a magma ocean
273 within the first few tens of million years after accretion (Abe, 1997) and it is tempting to
274 invoke it as the cause. The availability of Xe isotopes produced by short half-life decays
275 should make them suitable for more precisely constraining the timing of degassing (e.g.
276 Staudacher and Allègre 1982). However, uncertainties in the U/Pu of early Earth and
277 fission Xe isotope spectra need to be resolved before they can unequivocally identify
278 early Earth degassing (Boehnke et al. 2015).

279 The similarity of the atmospheric $^{38}\text{Ar}/^{36}\text{Ar}$ ratio with the chondritic value (0.188) (e.g. Ott,
280 2002), and an inability of kinetic fractionation to explain atmosphere Ne-Ar isotope
281 systematics (e.g. Marty, 2012), rules out significant loss of early Earth atmospheric noble
282 gases by hydrodynamic escape. It is commonly argued that the contribution of
283 primordial volatiles to Earth by comets until the Late Heavy Bombardment (LHB) at 3.8
284 Ga appears is limited (e.g. Dauphas et al. 2000), and mass balance calculations imply
285 that the atmospheric noble gas inventory requires a trivial contribution (Marty and
286 Meibom, 2007). However the concentration of noble gases in cometary material, and the
287 proportion of the material involved in the LHB that was cometary in origin, are both poorly
288 constrained.

289 The new degassing model requires that significant amounts of ^{40}Ar did not accumulate in
290 the Earth's atmosphere until after 4 Ga. As the K-rich continental crust is the dominant
291 source of degassing ^{40}Ar (e.g. Bender et al. 2008) the atmosphere accumulation history
292 can be used to place constraints on the growth history of the continental crust. The new

293 atmosphere outgassing history is consistent with models of continental crust growth that
294 requires initiation at around 4.0 Ga and slow continuous growth (e.g. Dhuime et al. 2012)
295 rather than early and rapid crust growth (e.g. Armstrong 1981) or late and rapid growth
296 (e.g. Taylor and MacLennan, 1985). This is not necessarily inconsistent with the earlier
297 formation of small volumes of K-poor basaltic crust, but does, however, support evidence
298 that large-scale differentiation of mantle and crust occurred several hundreds of million
299 years after Earth accretion (e.g. Kemp et al. 2010).

300

301 **5. Summary**

302 We have made high precision determinations of Ar isotopes trapped in the Devonian-
303 aged Rhynie chert from northeast Scotland. The $^{40}\text{Ar}/^{36}\text{Ar}$ intercept value (289.5 ± 0.4) is
304 a minimum of 3% lower than the modern air value, and is consistent with earlier studies
305 that demonstrates it has incorporated ancient atmospheric Ar. This new determination
306 requires that the Earth's atmosphere has accumulated $5 \pm 0.2 \times 10^{16}$ moles of ^{40}Ar in the
307 last 400 million years. The average rate ($1.24 \pm 0.06 \times 10^8$ mol $^{40}\text{Ar}/\text{year}$) overlaps the
308 rate determined from ice cores for the last 800,000 years (Bender et al. 2008), and
309 implies that there has been no resolvable temporal change in the rate of Earth
310 outgassing since the mid-Palaeozoic. The new data have been incorporated into the
311 Earth outgassing model of Pujol et al (2013) and offer precise constraints on the
312 evolution of the atmosphere $^{40}\text{Ar}/^{36}\text{Ar}$ and the differentiation history of solid Earth. The
313 model results require the degassing of the Earth's primordial volatiles in the first 100 Ma
314 after accretion. The atmosphere $^{40}\text{Ar}/^{36}\text{Ar}$ only started to increase significantly after 4
315 Ga, suggesting that major Earth differentiation occurred 100s million years after
316 accretion.

317

318 **Acknowledgements** FS and PMcC would like to express their gratitude to Grenville
319 Turner for stimulating their interest in this field many years ago. The work was funded by
320 NERC and SUERC. PG undertook the modeling while in receipt of a scholarship from
321 the Ecole Centrale Lyon. We are grateful to Ray Burgess and two anonymous reviewers
322 for their constructive input.

323

324 **References**

- 325 Abe, Y., 1997. Thermal and chemical evolution of the terrestrial magma ocean. *Phys.*
326 *Earth Planet. Int.* 100, 27-39
- 327 Allègre, C.J., Staudacher, T., Sarda, P., 1986/87. Rare gas systematics: formation of the
328 atmosphere, evolution and structure of the Earth mantle. *Earth Planet. Sci. Lett.*, 81,
329 127-150.
- 330 Allègre, C.J., Hoffman, A., O'Nions, R.K., 1996. The argon constraints on mantle
331 structure. *Geophys. Res. Lett.*, 23, 3555-3557.
- 332 Armstrong, R.L., 1981, Radiogenic isotopes: The case for crustal recycling on a steady-
333 state continental growth Earth. *Phil. Trans. Roy. Soc. London (A)* 301, 443–472.
- 334 Baron, M., Hillier, S, Rice, C.M., Czapnik, K., Parnell, J., 2004. Fluids and hydrothermal
335 alteration assemblages in a Devonian gold-bearing hot spring system, Rhynie,
336 Scotland. *Trans Roy. Soc. Edinburgh Earth Sci.* 94, 309-324.
- 337 Bender, M.L., Barnett, B., Dreyfuss, G., Jouzel, J., Porcelli, D., 2008. The contemporary
338 degassing rate of ^{40}Ar from the solid Earth. *Proc. Nat. Acad. Sci.* 105, 8232-8237.
- 339 Boehnke, P., Caffee, M.W., Harrison, T.M., 2015. Xenon isotopes in MORB source, not
340 distinctive of early global degassing. *Geophys. Res. Lett.* 42, 4367-4374.
- 341 Brown, H., 1949. Rare gases and the formation of the Earth's atmosphere. In *The*
342 *atmosphere of the Earth and the planets* G. Kuiper (Ed.) University of Chicago Press,
343 Chicago, 258-266.
- 344 Burnard, P.G., Stuart, F.M., Turner, G., Oskarsson, N., 1994. Air contamination of
345 basaltic magmas: implications for high $^3\text{He}/^4\text{He}$ mantle Ar isotopic composition *J.*
346 *Geophys. Res. Solid Earth* 99, 17,709-17,715.
- 347 Cadogan, P., 1977. Palaeoatmospheric argon in Rhynie chert. *Nature* 268, 38-40.
- 348 Davies, G.F., 1999. Geophysically constrained mantle mass flows and the ^{40}Ar budget: a
349 degassed lower mantle? *Earth Planet. Sci. Lett.*, 166, 149-162.
- 350 Dauphas, N., Robert, F., Marty, B., 2000. The late asteroidal and cometary
351 bombardment of Earth recorded in water deuterium to protium ratio. *Icarus* 148, 508–
352 512.
- 353 Dhuime, B., Hawkesworth, C.J., Cawood, P.A., Storey, C.D., 2012. A change in the
354 geodynamics of continental growth 3 billion years ago. *Science* 335, 1334–1336.
- 355 Fanale, F., 1971. A case for the catastrophic early degassing of the Earth. *Chem. Geol.*
356 8, 79-105.

357 Farley, K.A., Maier-Reimer, E., Schlosser, P., Broecker, W.S., 1995. Constraints on
358 mantle ³He fluxes and deep-sea circulation from an oceanic general circulation model.
359 J. Geophys. Res.: Solid Earth, 100, 3829–3839.

360 Gomes, R., Levison H.F., Tsiganis, K., Morbidelli, A., 2005. Origin of the cataclysmic
361 Late Heavy Bombardment period of the terrestrial planets. Nature 435, 466-469

362 Gonnermann, H.M., Mukhopadhyay, S., 2009. Preserving noble gases in a convecting
363 mantle, Nature, 459, 560-563.

364 Hanes, J.A., York, D., Hall, C.M., 1985. An ⁴⁰Ar/³⁹Ar geochronological and electron
365 microprobe investigation of an Archaean pyroxenite and its bearing on ancient
366 atmospheric compositions. Can. J. Earth Sci., 22, 947-958.

367 Hamano, Y., Ozima, M., 1978. Earth-atmosphere evolution model based on Ar isotopic
368 data. In: E.C. Alexander and M. Ozima (Editors), Terrestrial Rare Gases, Japan.
369 Science Society Press, Tokyo, Advances in Earth and Planetary Science, 3,155-171.

370 Honda, M., McDougall, I., Patterson, D.B., Douglis, A., Clague D.A., 1993. Noble
371 gases in submarine pillow basalt glasses from Loihi and Kilauea, Hawaii: a solar
372 component in the Earth. Geochim. Cosmochim. Acta 57, 859-874.

373 Kemp, A.I.S., Wilde, S.A., Hawkesworth, C.J., Coath, C.D., Nemechin, A., Pidgeon, R.T.,
374 Vervoort, J.D., DuFrane, S.A., 2010. Hadean crustal evolution revisited: New
375 constraints from Pb-Hf isotope systematics of the Jack Hills zircons. Earth Planet. Sci.
376 Lett., 296, 45-56.

377 Lee, J.Y., Marti, K., Severinghaus, K., Kawamura, K., Yoo, H.S., Lee, J.B., Kim, J.S.,
378 2006. A re-determination of the isotopic abundances of atmospheric Ar. Geochim.
379 Cosmochim. Acta 70, 4507-4512.

380 Mark, D.F., Barfod, D., Stuart, F.M., Imlach, J., 2010. The ARGUS multi-collector mass
381 spectrometer: performance for ⁴⁰Ar/³⁹Ar geochronology. Geochem. Geophys. Geosys.
382 10, 1-9.

383 Mark, D.F., Stuart, F.M., de Podesta, M., 2011a. New high-precision measurements of
384 the isotopic composition of atmospheric argon. Geochim. Cosmochim. Acta 75, 7494-
385 7501.

386 Mark D.F., Rice C.M., Fallick A.E., Trewin N.H., Lee M.R., Boyce A.J., Lee J.K.W.,
387 2011b. Ar/Ar dating of hydrothermal activity, biota and gold mineralization in the Rhynie
388 hot-spring system, Aberdeenshire, Scotland. Geochim. Cosmochim. Acta 75, 555–569.

389 Mark D.F., Rice C.M., Trewin N.H., 2013. Discussion on “A high precision U-Pb age
390 constraint on the Rhynie Chert Konservat-Lagerstätte: Time scale and other
391 implications,” J. Geol. Soc. London 170, 701-703.

392 Marty, B., 2012. The origins and concentrations of water, carbon, nitrogen and noble
393 gases on Earth. *Earth Planet. Sci. Lett.* 312, 56-66.

394 Marty, B., Meibom, A., 2007. Noble gas signature of the late heavy bombardment in the
395 Earth's atmosphere. *eEarth* 2, 43–49.

396 Nier, A.O., 1950. A re-determination of the relative abundances of the isotopes of
397 carbon, nitrogen, oxygen, argon and potassium. *Phys. Rev.* 77, 789-793.

398 O'Nions, R.K., Tolstikhin, I., 1996. Limits on the mass flux between lower and upper
399 mantle and stability of layering. *Earth Planet. Sci. Lett.*, 139, 213-222.

400 Ott, U., 2002. Noble gases in meteorites - trapped components. *Rev. Mineral. Geochem.*
401 62, 71–100.

402 Ozima M., Podosek, F., 1983. Noble gas geochemistry. Oxford University Press, pp 367.

403 Porcelli, D., Wasserburg, G.J., 1995. Mass transfer of helium, neon, argon, and xenon
404 through a steady-state upper mantle. *Geochim. Cosmochim. Acta* 59, 4921-4937.

405 Pujol, M., Marty, B., Burgess, R., Turner, G., Philippot, P., 2013. Argon isotopic
406 composition of Archaean atmosphere probes early Earth geodynamics. *Nature* 498,
407 87–90.

408 Renne, P.R., Swisher, C.C., Deino, A., Karner, D.B., Owens T.L., Depaolo, D., 1998.
409 Intercalibration of standards: absolute ages and uncertainties in $^{40}\text{Ar}/^{39}\text{Ar}$ dating. *Chem.*
410 *Geol.* 145, 117-152.

411 Rice, C., Ashcroft, W., Batten, D., Boyce, A., Caulfield, B., Fallick, A., Hole, M., Pearson,
412 M., Rogers, G., Stuart, F., Trewin, N. & Turner, G., 1994. The geology of an Early
413 Devonian hot spring system near Rhynie. *J. Geol. Soc. London*, 152, 229-250.

414 Staudacher, T., Allègre, C.J., 1982. Terrestrial xenology. *Earth Planet. Sci. Lett.* 60, 389-
415 406.

416 Stuart, F.M., Turner, G., 1992. The abundance and isotopic composition of noble gases
417 in ancient fluids. *Chem. Geol.* 101, 97-111.

418 Stuart, F.M., Turner, G., 1998. Mantle-derived ^{40}Ar in mid-ocean ridge hydrothermal
419 fluids: implications for the source of volatiles and mantle degassing rates. *Chem. Geol.*
420 147, 77-88.

421 Starkey, N.A., Stuart, F.M., Ellam, R.M., Fitton, J.G., Basu, S. & Larsen, L.M., 2009.
422 Helium isotopes in early Iceland plume picrites: Constraints on the composition of high
423 $^3\text{He}/^4\text{He}$ mantle. *Earth Planet. Sci. Lett.* 277, 91-100.

424 Taylor, S.R., McLennan, S.M., 1985. *The Continental Crust: Its Composition and*
425 *Evolution*: Oxford, Blackwell Scientific Publications, pp. 312.

- 426 Turcotte, D., Schubert, G., 1988. Tectonic implications of radiogenic noble gases in
427 planetary atmospheres. *Icarus* 74, 34-46.
- 428 Turekian, K., 1959. The terrestrial economy of helium and argon. *Geochim. Cosmochim.*
429 *Acta* 17, 37-43.
- 430 Turner, G., 1988. Hydrothermal fluids and argon isotopes in quartz veins and cherts.
431 *Geochim. Cosmochim. Acta* 52, 1443-1448.
- 432 Turner, G., 1989. The outgassing history of the Earth's atmosphere. *J. Geol. Soc.*
433 *London* 146, 147-154.
- 434

435 **Figure captions**

436

437 Figure 1. $^{40}\text{Ar}/^{36}\text{Ar}$ vs. $^{39}\text{Ar}/^{36}\text{Ar}$ isochron plot for the new analyses of Rhynie chert. The
438 data plot within a triangle identified by the grey dotted lines. The dashed line is the air
439 $^{40}\text{Ar}/^{36}\text{Ar}$ (298.8 ± 0.5 ; Lee et al. 2008). The full black line is the isochron determined
440 using the *Masspec* Ar isotope reduction software. The intercept at $^{39}\text{Ar}/^{36}\text{Ar} = 0$ defines a
441 palaeo-atmospheric $^{40}\text{Ar}/^{36}\text{Ar}$ of 289.5 ± 0.4 (MSWD = 1.3). The isochron age (380 ± 30
442 Ma) is indistinguishable from the age of the hydrothermal feeder vein. The yellow data
443 are excluded when they do not overlap the isochron at 2σ level; they can be most readily
444 explained by the presence of excess ^{40}Ar derived from the hydrothermal fluids (e.g.
445 Stuart and Turner, 1992). Uncertainties are 2σ .

446

447 Figure 2. Plot shows the deviation of Ar isotope composition of unirradiated Rhynie chert
448 from modern atmosphere ($\delta^{38}\text{Ar} = 0$, $\delta^{40}\text{Ar} = 0$). The yellow circles are the total gas
449 released by step-heating chert fragments, and the clear circles are the single-step
450 fusions of small fragments (see SI Table 2). All uncertainties are 2σ . Delta values have
451 been determined from:

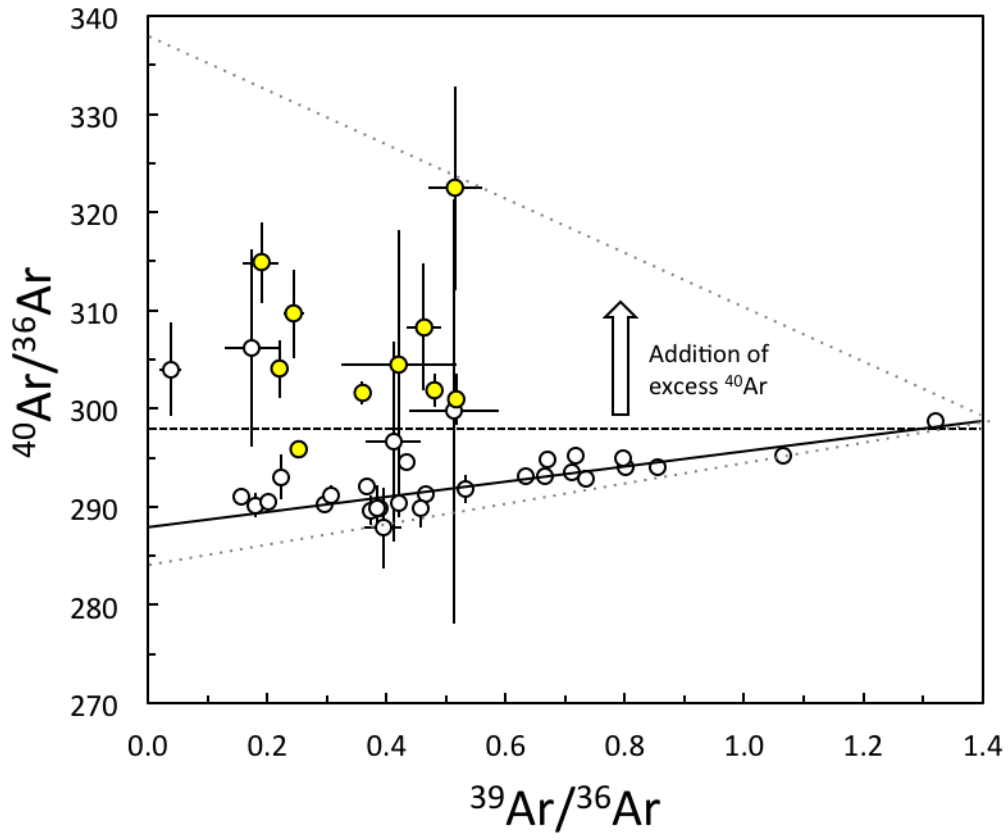
452
$$\delta^x\text{Ar} = 1000 \times ({}^x\text{Ar}/^{36}\text{Ar}_{\text{measured}} - {}^x\text{Ar}/^{36}\text{Ar}_{\text{air}})/({}^x\text{Ar}/^{36}\text{Ar}_{\text{air}})$$

453

454 Figure 3. Plots showing the evolution of the atmosphere $^{40}\text{Ar}/^{36}\text{Ar}$ ratio versus time,
455 constrained using the box model (see text and Supplementary Information). The blue
456 curves represent modeled history derived from this work. The black curves represent the
457 extremes of crustal degassing constrained from Pilbara quartz (Pujol et al., 2013). The
458 upper panel shows atmosphere evolution over all of Earth history, and the lower panel
459 shows the last 500 million years. The grey bars at 3.5 Ga and 404 Ma record the
460 extrapolated atmospheric $^{40}\text{Ar}/^{36}\text{Ar}$ of Pujol et al. (2013) and this work respectively.

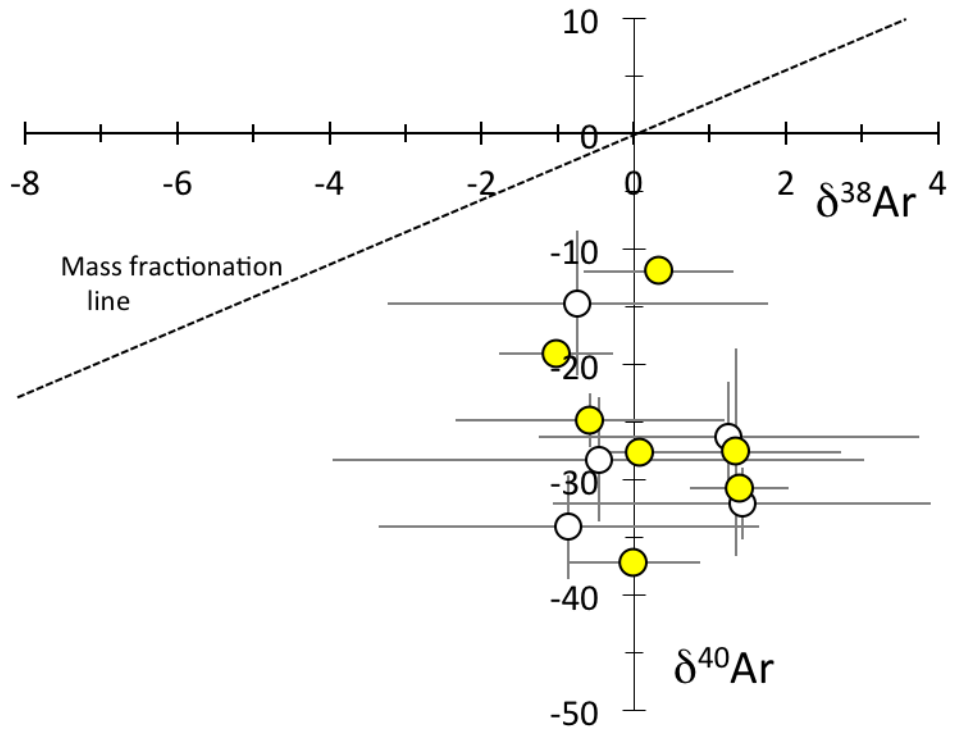
461

462



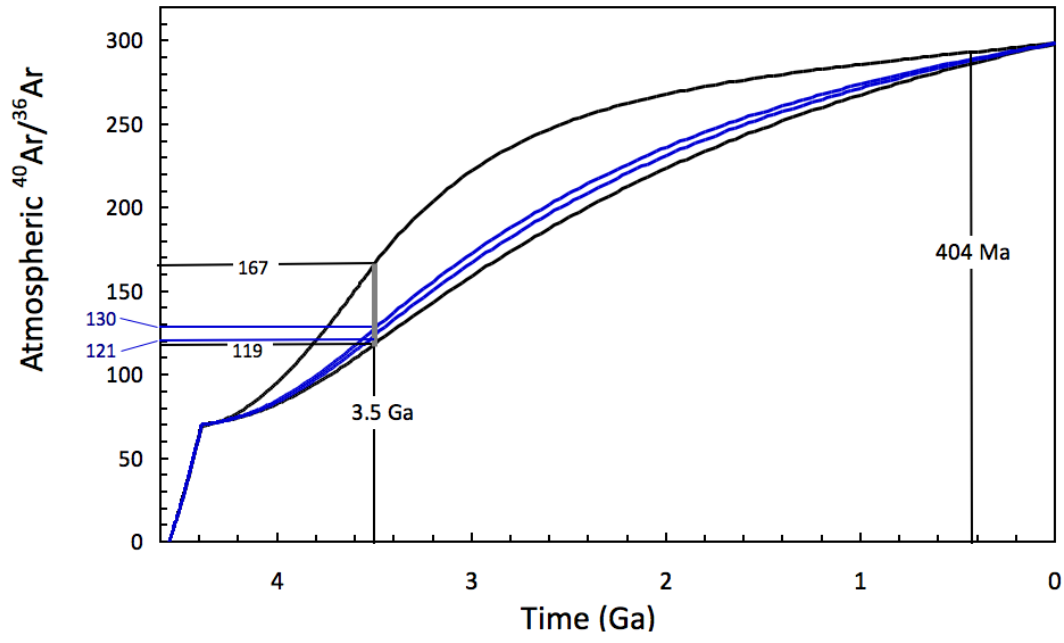
463
 464
 465
 466
 467
 468

Figure 1: Stuart et al.

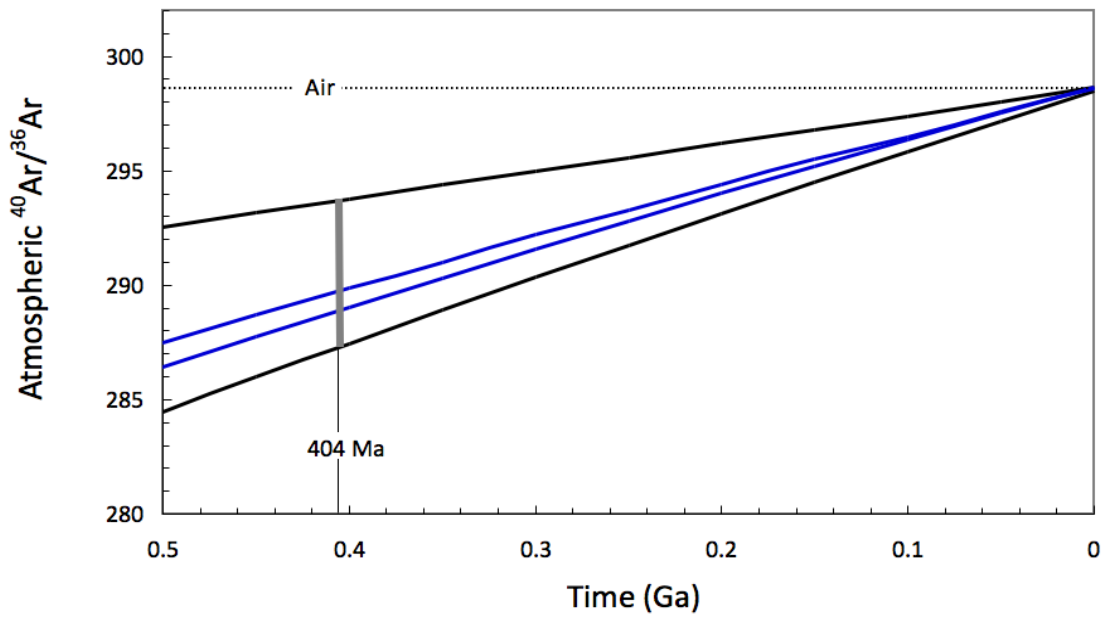


469
 470
 471 Figure 2: Stuart et al.
 472

473
474



475
476



477
478
479
480
481
482

Figure 3 Stuart et al.